Telemanipulation over the Internet: a Tele-Assembly Experiment

Bartlomiej Stanczyk, Sandra Hirche and Martin Buss
Institute of Automatic Control Engineering
Technische Universität München
D-80290 München, Germany
{Sandra.Hirche, Bartlomiej.Stanczyk, Martin.Buss}@ei.tum.de

Abstract— **To achieve stable and transparent telemanipulation, one needs to overcome the common communication problems and assure a compliant motion of the telemanipulator in the remote environments. This paper addresses i) stability conditions for the application in packet switched networks with time varying communication latencies and packet loss, as e.g. the Internet, and discusses the impact of the packet processing protocol on the stability and the performance, and ii) investigates the manipulation and control problems of a teleoperated redundant manipulator, equipped with a stiffness control algorithm.**

I. INTRODUCTION

The goal of multimodal telemanipulation also called telepresence systems is to enable a human operator to actively perform complex manipulation tasks in possibly distant or differently scaled remote environment. Application areas reach from telemanufacturing and telemaintenance to telesurgery and rescue applications.

A multimodal telepresence system is shown in Fig. 1. The human operator manipulates the force feedback capable Human System Interface (HSI) thereby commanding the executing robot (teleoperator). While the teleoperator interacts with the usually unknown remote environment the sensor data (visual, auditory, haptic) are fed back and displayed to the operator.
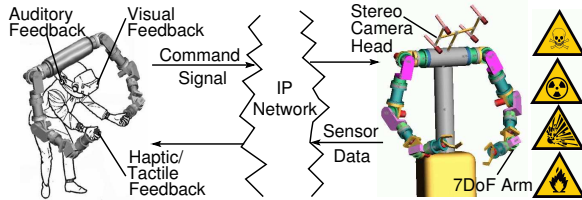

Fig. 1. Multimodal human rescuing telepresence system.

The sampled command signals and sensor data, both continuously generated realtime mediastreams, are communicated via a packet switched communication network, e.g. the Internet, thereby closing a global control loop. Substantial time varying delays as they occur in the Internet destabilize the closed loop system resulting in a severe hazard to the safety of the human and the remote environment.

Stability of haptic telepresence with time delay can be guaranteed by applying the passivity concept. The resulting control methods, as the scattering transformation and the combined velocity/force control of teleoperator/HSI, see [1], stabilize the system for arbitrary but constant delay; in the extension also for time varying delays, see [2], [3]. The

stability conditions are formulated for the continuous time case, hence do not incorporate the effects of a packet switched communication network.

In such a network depending on the traffic conditions the data packets are randomly delayed, may arrive in permutated order, and packet loss may occur. Packet loss or increasing time delay may result in a buffer underrun at the receiver side. Keeping the old value (Hold Last Sample) or generating a new value with estimated data, see [4], have been successfully applied in networked control systems (NCS). These compensation strategies are not passive in general but can be passfied, see [5].

Another requirement for stability and transparency of a telepresence system is the proper construction and control of the manipulator used on the remote side. It is possible to summarize the design requirements as a simple reproduction of the human manipulation abilities. The resulting kinematic design is a 7 degree-of-freedom (DOF) arm with large, convex, human sized workspace. Since the arm is kinematically redundant, there is a need of applying a redundancy resolution strategy, which does not require inverting of the manipulator Jacobian neither for motion nor for dynamic control. The extended task space formulation of [6] is a good choice for a position based self motion parametrization. The necessity of compliant motion in teleoperation scenarios was reported in many previous works. The main challenge here is to avoid large forces, which occur while contacting the remote environment. The strategy applied in this work bases on stiffness control, see e.g. [7].

This paper focuses on the experimental evaluation of the control strategies aiming at stable haptic telepresence over the Internet with a redundant teleoperator. As a benchmark a 2DOF tele-assembly experiment is performed.

The paper is organized as follows: section 2 introduces passivity based stabilization methods and measures of transparency; in section 3 the passivity of packet processing algorithms and the benefit of the position/velocity/force architecture is analyzed; section 4 describes the design and control of the telemanipulator; the last two sections present the experimental system architecture and the results.

II. PASSIVITY BASED GLOBAL CONTROL ARCHITECTURE

The human rescuing telepresence system basically consists of a force feedback capable HSI (variables indexed $_h$) and the teleoperator (index $_t$) interacting with an usually unknown

remote environment (index e) as shown in Fig. 2. In bilateral telepresence the human manipulates the HSI applying the force f_h. Based on stability arguments in the standard architecture the HSI velocity $\dot{x}_h$ is communicated to the teleoperator where the local velocity control loop ensures the tracking of the desired teleoperator velocity $\dot{x}_t^d$ (d denotes desired). The force f_e sensed at the remote site, resulting from the interaction with the environment, is transmitted back to the HSI serving as reference signal f_h^d for the local force control.

The HSI and the teleoperator are connected through a communication network closing a global control loop via the human operator. In case of a packet switched unreliable service network, as e.g. the Internet, the data packets, thus the control signals are afflicted with varying time delay and packet loss. Without further control measures the closed loop system is unstable.

A. The Passivity Approach

A common approach to analyze and synthesize telepresence system architectures with time delay is the passivity concept providing a sufficient condition for stability of the haptic telepresence system. A complex system of interconnected network elements (n-ports) is passive if each of the subsystems is passive. A passive element is one for which, given zero energy storage at $t = 0$, the property

$$\int_0^t P_{in}(\tau)\,\mathrm{d}\tau = \int_0^t u^T(\tau)y(\tau)\,\mathrm{d}\tau \geq 0 \quad \forall t > 0 \qquad (1)$$

holds, with $P_{in}(\tau)$ denoting the power stored or dissipated in the system, $u(\tau)$, $y(\tau)$ being the input and output vector. In classical telepresence architectures, as proposed in [1], the appropriately locally controlled HSI and teleoperator exchange velocity and force signals, as the mapping from velocity to force is generally passive, hence the teleoperator and the HSI are passive subsystems. The environment is considered passive and it is assumed that the (possibly so trained) human operator behaves in a cooperative, i.e. passive way.

If the communication between HSI and teleoperator is delayed by $T_1(t)$, $T_2(t)$ in the forward and the backward path, respectively, then it is straightforward to show that the communication line generates energy, hence is not passive. The scattering transformation first applied to telepresence systems in [1] passifies the communication two-port for *constant* delays $T_1(t) = T_1$, $T_2(t) = T_2$ with the wave variable transformation

$$\begin{aligned} u_l &= \frac{1}{\sqrt{2b}}(f_h^d + b\dot{x}_h); \quad u_r = \frac{1}{\sqrt{2b}}(f_e + b\dot{x}_t^d); \\ v_l &= \frac{1}{\sqrt{2b}}(f_h^d - b\dot{x}_h); \quad v_r = \frac{1}{\sqrt{2b}}(f_e - b\dot{x}_t^d). \end{aligned} \qquad (2)$$

Using the notation of (1) the input vector is given by $u^T = [\dot{x}_h \; -\dot{x}_t^d]$ and the output vector by $y^T = [f_h^d \; f_e]$. Disregarding the blocks $f_1(t)$, $f_2(t)$ and the position feedforward in Fig. 2,
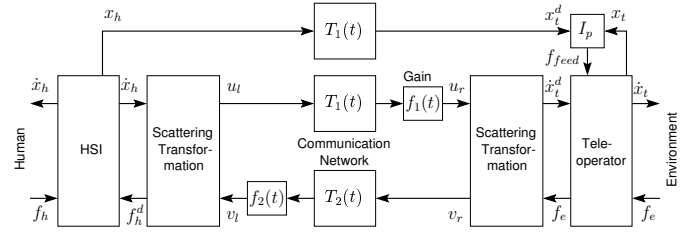

Fig. 2. Transparency orientated system architecture for time varying delay with time varying gains $f_1(t), f_2(t)$ and additional position feedforward.

the communication two-port now becomes passive, i.e. does not generate energy

$$\int_0^t P_{in}(\tau)\,\mathrm{d}\tau = \int_0^t (\dot{x}_h f_h^d - \dot{x}_t^d f_e)\,\mathrm{d}\tau \geq 0 \quad \forall t. \qquad (3)$$

If the delay varies over time the passivity condition for the communication two-port/scattering transformation may be violated depending on the rate of change of the delay as shown in [2]. At times when the time delay increases, i.e. the rate of change of the time delay is positive $\dot{T}_i(t) > 0$ the communication line generates energy, thus is not passive. At decreasing time delay $\dot{T}_i(t) < 0$ the communication line dissipates energy, hence is passive.

In order to preserve passivity the time varying gains $f_i^2(t) \leq 1 - \dot{T}_i(t)$, $i = 1, 2$ are inserted shaping the energy output of the communication two-port depending on the rate of change of the transmission delay as shown in Fig. 2. For constant delay the gains calculate to $f_1 = f_2 = 1$ recovering the results of [1].

B. Transparency

Ideal kinesthetic coupling expressed in the notion of *transparency* is achieved if the human operator feels directly connected to the remote environment. According to [15] this requires the positions and forces at the HSI and teleoperator to be equal
$$x_h = x_t \quad \wedge \quad f_h = f_e. \qquad (4)$$

In the time varying delay case the passifying gains $f_1(t)$, $f_2(t)$ transform the signals and thereby cause loss of transparency. Then a position drift between HSI and teleoperator may occur that is non-recoverable as velocity control cannot guarantee steady state error free position tracking. In order to overcome this deficiency an additional position feedforward is proposed in [3]. The position error $e(t) = x_h(t - T_1(t)) - x_t(t)$ is weighted by feedforward gain I_p acting as a proportional position controller with the (if necessary) saturated control output $f_{feed}(t) = I_p\mathrm{sat}_p(e(t))$, see Fig. 2. The gain I_p and the saturation p are chosen so that the non-passivity of the position feedforward is compensated by the excess passivity of the teleoperator, for more details see [3].

III. COMMUNICATION OVER PACKET SWITCHED NETWORKS

We now consider a sampled data system for HSI and teleoperator and a dynamically routed multi-path packet switched network with time varying delay and packet loss, as e.g.

the Internet, for communication. The communication line is decomposed into the packeting at the sender side, the packet transmission, and the packet processing algorithm at the receiver side, see Fig. 3.
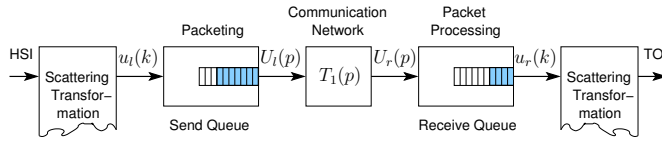

Fig. 3.   Communication network with packet processing algorithms.

Discrete scattering transformation is applied at the sender and the receiver side using the transformation equations given by (2) in discrete time now with the independent variable k. We assume that the sender as well as the receiver side operate with the same sampling interval T_A and that the sampled data packets are sent in equal fixed time intervals over the network. In general a fixed number L of consecutive samples of the wave variables $u_l(k)$ representing the output of the scattering transformation, are packed into one IP-packet $U_l(p)$ and put on the outgoing link.

During transmission over the network the IP-packet $U_l(p)$ experiences a load and routing policy dependent time varying link delay of $T_1(p)$. Additionally in a congested network IP-packets are discarded at the congested receive queues of intermittent routers resulting in packet loss.

A. Packet Processing: Use Freshest/ Hold Last Sample

Varying time delay can be compensated through queueing as in [8]; then all data packets experience the worst case but constant delay of the system. As a result the performance of the haptic telepresence system is degraded by the additional virtual delay. Here the Use-Freshest-Sample (UFS) algorithm without any buffering of data packets is applied here. Only the youngest packet is processed next, older packets, arriving too late are discarded. This strategy is passive, as shown in [5]. The effective communication delay of the packets is not increased by the UFS strategy, but additional packet loss is induced.

The processing induced packet loss as well as the network induced loss result in empty sampling instances at the receiver. The missing data can be estimated. A very simple estimation strategy is the Hold-Last-Sample (HLS) strategy. In case that there is no more data packet in the receive queue, the last sample is held until the next younger packet arrives. The HLS algorithm is not passive in general, see [5] for the proof.

B. Tracking Improvement by Position Feedforward

The position/velocity/force architecture has successfully been applied in the continuous time case improving the position tracking of HSI and teleoperator, see [3]. Now we investigate the applicability in a packet switched network, where the position information x_h is transmitted in the same data packet as the wave variable u_l. The UFS/HLS algorithm is applied to the wave variable and to the position feedforward
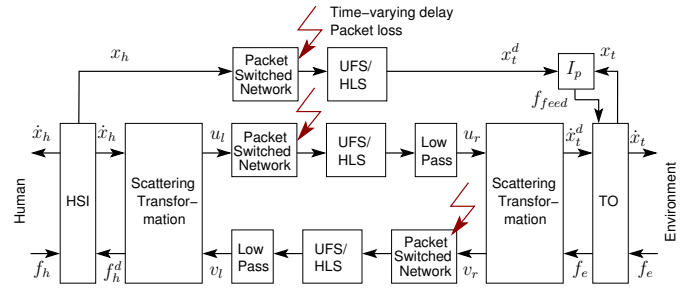

Fig. 4.   Position feedforward architecture with combined UFS/HLS low pass filtering strategy in packet switched networks.

signal, see Fig. 4. In order to preserve passivity and to cancel out wave reflections, the wave variables are filtered by low passes as proposed in [5]. The packeting algorithm for the position feedforward signal in this architecture has no effect on passivity as it is guaranted by the saturation of the feedforward controller output.

Simulations are performed in order to analyze the effect of the position feedforward with single applied HLS in the forward path. The teleoperator moves in free space with a small environment damping $b_e = 0.1$. The delays in the forward and backward paths are kept constant $T = 100$ms. The HLS algorithm distorts the signal and induces wave reflections as shown in Fig. 5(a), where the outgoing signal $u_r(t)$ before and after the HLS is depicted.
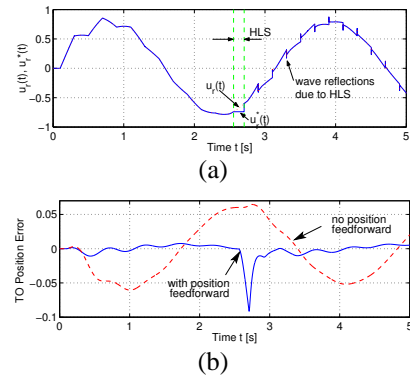

Fig. 5.   Input and output signal of single applied HLS (a) and position tracking of the teleoperator with and without position feedforward (b)

The tracking error $e(t) = x_h(t - T) - x_t(t)$ is depicted in Fig. 5(b). Without position feedforward there is a considerable tracking error, after the HLS a tracking error offset can be noticed. With position feedforward control the position error is reduced and only temporarily increased due to the position HLS, more intelligent packet processing algorithms are necessary to keep the error all the time at the same low value. In general the position/velocity/force architecture reveals good performance in terms of position tracking compared to the standard velocity/force architecture.

IV. TELEOPERATOR DESIGN AND CONTROL

The remarkable dexterity that humans exhibit in various manipulation tasks is mainly due to i) the kinematic re-

dundancy of the arm and ii) the ability to adapt the limb stiffness/compliance to the current task and iii) the presence of two arms. To achieve transparent and intuitive telepresence, the manipulator placed on the remote site has to reveal the same physical characteristics as the actual limbs of the operator.

Another important requirement is that the manipulator control strategy should be robust against the problem of singularities, which pose major difficulties in Cartesian control schemes based on the Jacobian inverse. Especially, in teleoperation scenarios, when the user is liable to unintentionally drive the slave robot toward/through a singularity. That is why strategies are preferred that do not involve Jacobian inversion neither for trajectory generation nor for dynamic control.

A. Manipulator Kinematics

The telemanipulator consists of a human-scaled arm, see subsection C for construction details. A kinematic analysis of human limbs reveals that the minimum number of DoFs used for their modeling is 7 (there exist approaches representing human arms as a 7, 8, 10 or more DoFs). Although the kinematical structure of the human operator and the slave robot do not need to match exactly, a 7 DoF structure is chosen as a trade-off between system complexity and performance. Investigations of possible 7 DoF structures result in the design shown in Fig. 6, which is proven to be optimal [9]. The resulting design consists of two spherical joints with three DoFs at the shoulder and the wrist, and one rotational joint at the elbow. The Denavit-Hartenberg (DH) parameters for the arm with the corresponding set of frames are listed in Table I. The analysis of the resulting workspace shows that
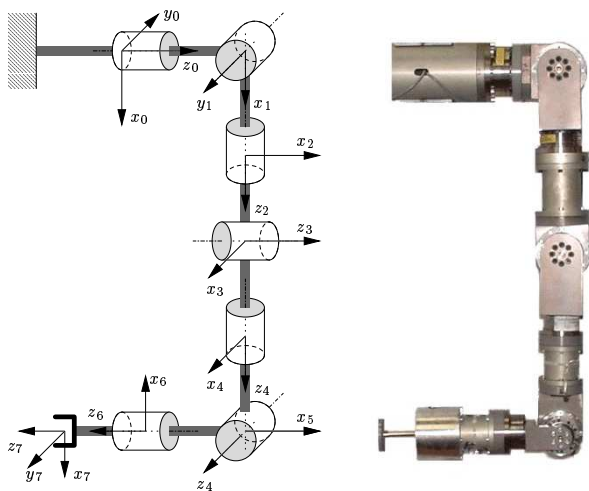

Fig. 6.   Schematic picture of the arm

the kinematic properties do not suffer from choosing only one degree of redundancy, due to the increased angle ranges in joint space.

In case of redundant manipulators, the inverse kinematic (IK) problem is solved usually on the velocity level using the

TABLE I
TELEOPERATOR DENAVIT-HARTENBERG PARAMETERS

Joint nr i	Link offset a_i	Link length l_i [m]	Link twist α_i [rad]
1	0	0	$\pi/2$
2	0	0	$\pi/2$
3	0	0.312	$-\pi/2$
4	0	0	$\pi/2$
5	0	0.312	$-\pi/2$
6	0	0	$\pi/2$
7	0	0.244	$\pi/2$

Jacobian inverse method

$$\dot{q} = \tilde{J}^{-1}\dot{X}, \qquad (5)$$

where $Y = [x, y, z, \alpha, \beta, \gamma]^T$ is the task space vector, q is the 7×1 joint space vector and $\tilde{J}$ is is the 6×7 manipulator Jacobian. The Jacobian inverse $\tilde{J}^{-1}$ is chosen in a way that a scalar objective function of the joint variables is minimized [10]. Such a solution though is sensitive to both mechanical and algebraic singularities and requires special care. That is why redundancy resolution on the position level is proposed.

Although the manipulator is kinematically redundant, there exists a closed form solution for the inverse kinematics (IK) problem [11], [6] (for a detailed description see [12]). It is based on the extension of the task space vector Y with an additional variable θ, the so called "elbow angle", which in this case has the following physical meaning: if the positions of the shoulder s, the wrist w and the end-effector d are fixed, the elbow e is free to swivel about the axis from the shoulder to the wrist, as shown in Fig. 7. This phenomenon, called
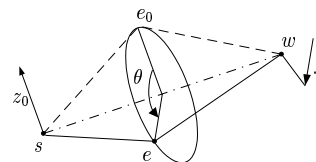

Fig. 7.   The elbow angle θ definition

"orbiting" in the literature, is the arm null space movement. The elbow position on the circle can be determined by specifying the angle between the arm projection of an arbitrary reference position e_0 and the actual position e onto the circle plane. In this case, $\theta = 0$ if the plane spanned by the points s, e and w includes the z_0 vector of the world coordinate system. The angle θ parameterizes the null space motion of the manipulator uniquely, so that the IK function is given as a function of the extended task space vector $x = [Y, \theta]^T$. The resulting manipulator Jacobian J is now redefined as a 7×7 matrix

$$\dot{x} = J\dot{q} = \begin{bmatrix} \tilde{J} \\ J_\theta \end{bmatrix} \dot{q} \qquad (6)$$

The Y trajectory is generated by the user, while the θ trajectory has to be generated autonomously by a trajectory planner optimizing a local objective function.

B. Manipulator Control

For real world applications, when the robot has to interact with the physical environment, it is necessary to specify the suitable compliant behavior in Cartesian space. The motivation to use a compliant control algorithms as an alternative to a stiff position control is also proposed by other researchers [?], [13]. The main reason is to avoid large forces which result when a stiff robot arm comes in contact with the environment, especially if it is unknown and unstructured. A well established framework to achieve this goal is impedance control [14] that controls the dynamic relationship between the manipulator and environment by establishing a mass-spring-damper system relation between the Cartesian position x and the Cartesian force f:

$$f = M_k \ddot{x} + D_k \dot{x} + K_k x,$$

where M_k, D_k and K_k are virtual Cartesian inertia, damping and stiffness. In other words, the goal of impedance control is to mask the natural properties of the robot and to replace them with the specified mechanical impedance. An important assumption is being made at this point. The teleoperator control should incorporate the stiffness and damping part, but it should not reveal any inertial properties. The manipulator should work as a massless robot, and the user should feel only the inertia of the currently used tool, or transported loads. The control strategy chosen here is based on an extension of stiffness control [7]. It makes use of the idea of mapping the Cartesian matrices K_k and D_k into the joint space K_j and D_j, using the extended geometrical Jacobian J:

$$K_j = J^T K_k J$$
$$D_j = J^T D_k J$$

In case of a 7 DoF manipulator, K_k and D_k are 7×7 diagonal matrices corresponding to the desired stiffness/damping in task space coordinates (three translational, three rotational and θ parameter), so that the the null space dynamic behavior is also controlled. The 7×7 D_j and K_j matrices are then intentionally non-diagonal. Having compensated the natural dynamics of the manipulator, the control law is given by

$$J^T K_k J \Delta q_e + J^T D_k J \Delta \dot{q}_e = \ddot{q}_d$$
$$M(\ddot{q}_d) + H(q, \dot{q}) + G(q) = \tau$$

where Δq_e and $\Delta \dot{q}_e$ are the position and velocity error in joint space, M the is manipulator inertia matrix, $H(q, \dot{q})$ is the torque resulting from Coriolis, centrifugal and friction forces, $G(q)$ is the gravity part, and τ is the motor torque. The chosen control strategy requires neither inversion of the manipulator Jacobian, nor of the manipulator inertia matrix. The corresponding block diagram is shown in Fig. 8, where $x^d, \dot{x}^d, q^d, \dot{q}^d$, are the desired position and velocity trajectories in Cartesian and joint space, and IK is the inverse kinematics solution. The blocks P_-^+ and D_-^+ are responsible for keeping the joint space PD gains within a stability range, as well as for assuring empirically established minimal gains able to act against friction modeling errors.
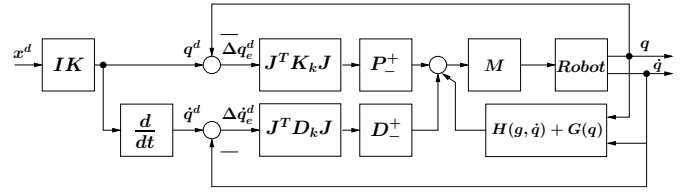

Fig. 8.   Stiffness control block diagram

C. Hardware and Implementation Details

The arms are built using commercially available components together with aluminium/steel construction elements. The arm reach (shoulder to force/torque sensor) is 0.86 m, weight in total approx. 13.5 kg, "worst case" payload is 6 kg. The motors are Maxon motors type RE40, gears Harmonic Drive type HFUC-25-160 (joint 1), HFUC-20-160 (joints 2 to 4) and HFUC-17-100 (joint 5 to 7). The motor torques are controlled by PWM amplifiers, operating in current control mode with the reference given by a voltage from the D/A converter output of the I/O board (Sensoray 626). The position of each joint is measured by an optic pulse incremental encoder on the motor shaft and then processed by a quadrature encoder on the I/O board. The force/torque is measured using a JR3 force/torque sensor. The control loops are composed of MATLAB/SIMULINK blocksets; standalone realtime code for RT Linux is automatically generated from the SIMULINK model.

V. TELEMANIPULATION EXPERIMENT

The goal of the experiment is to screw a bolt into a wall in Berlin by means of the HSI located in Munich. Additionally, to the haptic also visual and auditive feedback is provided at the operator station.

A. Experimental System Architecture

The experimental setup, see Fig. 9, consists of the HSI, two single degree of freedom force feedback paddles and the teleoperator, the 7 DOF arm described above, each connected to a PC for control. The right hand paddle controls the Cartesian y-direction, hence the approach of the bolt to the wall. The left hand paddle controls the turning around the y-axis.
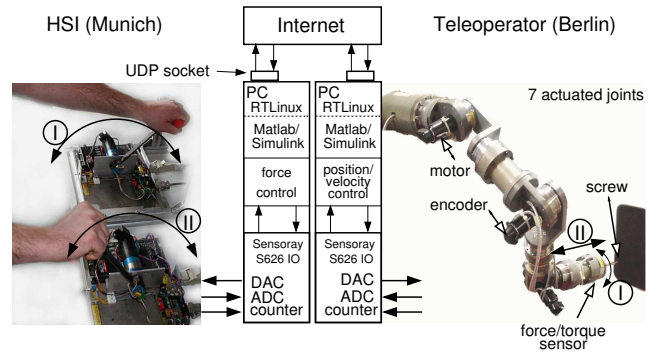

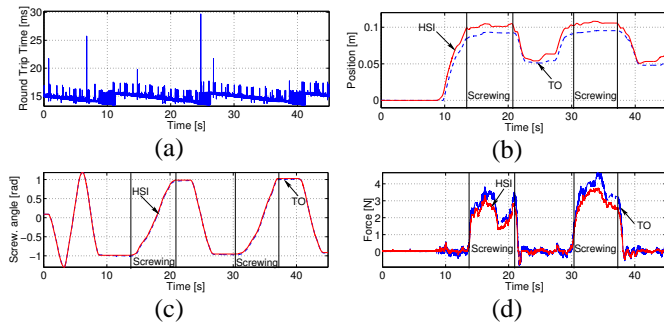Fig. 9.   Experimental system architecture.

Fig. 10. Experimental results: Round trip time delay (a), *y*-position (b) and force (d) tracking and screw angle tracking (c)

According to the proposed global control architecture in Fig. 4 the HSI is force controlled and the teleoperator is under stiffness control using velocity and position as reference. Both, the HSI and the 7 DOF arm operate at a sampling rate of 500 Hz. The output of the scattering transformation and the HSI position, see Fig. 4 is sent over a UDP socket connection, with one UDP packet containing one sample, thus the sampling rate of the communication network is equal to the sampling rates of the local control loops. A first order low pass with a gain of one and a cut frequency of 10 Hz is used as passivating filter, see Fig. 4.

B. Experimental Results

The mean round trip delay of the UDP connection Munich-Berlin is approximately 15 ms, its development over time is shown in shown in Fig. 10(a). The regular pattern is likely to be a result of the routing policies of intermittent routers. Both, the position and the force tracking of the approach is presented in Fig. 10(b) and (d), respectively. The force tracking shows very good results, further controller tuning at the teleoperator site is likely to further improve the position tracking. The screwing angle tracking is shown in Fig. 10(c), which is excellent.

In a second experiment the roundtrip delay is artificially increased to approximately 200 ms. The results in terms of position and force tracking for the approach and the screwing are presented in Fig.11 validating the proposed approach. The video of the experiment is available under `http://www.lsr.ei.tum.de/movies`.
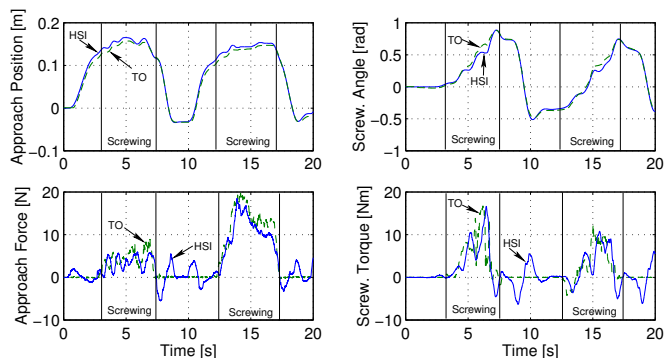

Fig. 11. Experimental results: position and force tracking

VI. CONCLUSIONS

Aiming at multi degree-of-freedom (DOF) telemanipulation over the Internet two of the major challenges are addressed in this paper, namely stability and performance in presence of time-varying time delay and packet loss in the communication and the compliance control of a redundant teleoperator. The packet processing algorithm Use freshest/ Hold last sample (UFS/HLS) combined with low pass filtering and stiffness control is applied to the 7 DOF human arm like teleoperator. The control architecture is validated in an assembly experiment with two degrees-of-freedom over the Internet. Future work is to investigate complex assembly experiments with more degrees-of-freedom at the HSI.

REFERENCES

[1] R. Anderson and M. Spong, "Bilateral Control of Teleoperators with Time Delay," *IEEE Transaction on Automatic Control*, vol. 34, pp. 494–501, 1989.
[2] N. Chopra, R. Lozano and M. Spong, "Passivation of Force Reflecting Bilateral Teleoperators with Time Varying Delay," in *Proceedings of the 8. Mechatronics Forum*, (Enschede, Netherlands), 2002, pp. 954-962.
[3] N. Chopra, M. W. Spong, S. Hirche, and M. Buss, "Bilateral Teleoperation over Internet: the Time Varying Delay Problem," in *Proceedings of the American Control Conference*, (Denver, CO), 2003, pp. 156–160.
[4] J. Nilsson, "Real-time Control Systems with Delays," PhD thesis , Lund Institute of Tecnology, 1998.
[5] S. Hirche and M. Buss, "Packet Loss Effects in Passive Telepresence Systems," in *Proceedings of the 43rd IEEE Conference on Decision and Control CDC 2004*, (Bahamas), 2004, *to appear*.
[6] H. Seraji, M. K. Long, and T. Lee, "Motion coontrol of 7-dof arms: The configuration control approach," *IEEE Transactions on Robotics and Automation*, vol. 9, no. 2, pp. 125–139, 1989.
[7] M. Mason and J.K. Salisbury, *Robot Hands and the Mechanics of Manipulation*. MIT Press, 1985.
[8] K. Kosuge and H. Murayama and K. Takeo, "Bilateral Feedback Control of Telemanipulators via Computer Network," in *Proceedings of the IEEE/RSJ International Conference on Intelligent Robots and Systems IROS*, 1996, Osaka, Japan, pp. 1380–1385.
[9] J. M. Hollerbach, "Optimum kinematic design for a seven degree of freedom manipulator," *Int. J. Robotics Research*.
[10] Y. Nakamura, *Advanced Robotics: Redundancy and Optimization*. Addison-Wesley, 1991.
[11] J. U. Korein, *A Geometric Investigation of Reach*. The MIT Press, 1985.
[12] B. Stanczyk, "Wrist-partitioned inverse kinematic solution for antropomorphic robotic arm," *Technical Report Control Systems Group*, June 2002.
[13] Y. Yokokohji and T. Yoshikawa, "Bilateral control of master-slave manipulators for ideal kinesthetic coupling-formulation and experiment," *Robotics and Automation, IEEE Transactions on*, vol. 10, no. 1042-296X, pp. 605–620, 1994.
[14] N. Hogan, "Impedance control: An approach to manipulation, part i - theory, part ii - implementation,part iii - applications," *Journ. of Dyn. Systems, Measurement and Control*, 1985.
[15] Y. Yokokohji and T. Yoshikawa, "Bilateral Control of Master-Slave Manipulators for Ideal Kinesthetic Coupling Formulation and Experiment," *IEEE Transactions on Robotics and Automation*, vol. 10, pp. 605–619, October 1994.
[16] M. Buss, "Multi-Fingered Regrasping Using a Hybrid Systems Approach," in *Proceedings of the 2nd IMACS/IEEE International Multiconference on Computational Engineering in Systems Applications (CESA'98)*, vol. 4, (Hammamet, Tunisia), pp. 857–861, 1998.